Quantum Routing of Single Photons with a Cyclic Three-Level System

Lan Zhou (周兰),[1] Li-Ping Yang (杨立平),[2] Yong Li (李勇),[3] and C. P. Sun (孙昌璞)[3,*]

[1]*Department of Physics and Key Laboratory of Low-Dimensional Quantum Structures and Quantum Control of Ministry of Education, Hunan Normal University, Changsha 410081, China*

[2]*State Key Laboratory of Theoretical Physics, Institute of Theoretical Physics, University of Chinese Academy of Science, Beijing 100190, China*

[3]*Beijing Computational Science Research Center, Beijing 100084, China*

(Received 21 March 2013; published 4 September 2013)

We propose an experimentally accessible single-photon routing scheme using a $\triangle$-type three-level atom embedded in quantum multichannels composed of coupled-resonator waveguides. Via the on-demand classical field being applied to the atom, the router can extract a single photon from the incident channel, and then redirect it into another. The efficient function of the perfect reflection of the single-photon signal in the incident channel is rooted in the coherent resonance and the existence of photonic bound states.

DOI: 10.1103/PhysRevLett.111.103604 PACS numbers: 42.50.Ex, 03.65.Nk, 03.67.Lx, 78.67.−n

Scalable quantum information processing in quantum computation and communication is essentially based on a quantum network. A key element inside is the quantum node, which coherently connects different quantum channels. It is called a quantum router for controlling the path of the quantum signal with fixed Internet Protocol (IP) addresses, or called a quantum switch without fixed IP addresses.

Recently, many theoretical proposals and experimental demonstrations of a quantum router have been carried out in various systems, i.e., cavity QED system [1], circuit QED system [2], optomechanical system [3], and even a pure linear optical system [4,5]. The essence lying at the core is the realization of the coupling between a two- (or few-) level system and quantum channels [6–10]. We notice that, except for the experiment in Ref. [5] implemented with linear optical devices, the quantum router demonstrated in most experiments and theoretical proposals has only one output terminal. Thus the ideal quantum router with multiaccess channels deserves more exploration.

In this Letter, we theoretically propose a scheme for quantum routing of single photons with two output channels, which are composed of two coupled-resonator waveguides (CRWs). The quantum node is realized by a three-level system with three transitions forming a cyclic ($\triangle$-type) structure [11–14]. To locate the different IP addresses, two different transitions of the $\triangle$ atom are coupled to the photonic modes of the two channels respectively and the other is used to connect the two channels with a classical field. We study the single-photon scattering in this proposed hybrid system. It is shown that the quantum node indeed works as a multichannel quantum router since the classical field can redirect single photons into different channels. The total reflections are guaranteed by the existence of quasibound states due to the coupling of a discrete energy level and a continuum. Actually, there have been numerous theoretical studies [15–20] focusing on the von Neumann–Wigner conjecture [21]: whether or not there exist (quasi-) bound states when discrete energy levels are coupled to a continuum. Now, our hybrid system provides a platform to probe this kind of bound states.

Quantum node with $\triangle$-type atom.—The considered system (see Fig. 1) consists of two one-dimensional (1D) CRW channels whose cavity modes are described by the creation operators $a_j^\dagger$ and $b_j^\dagger$, respectively, and a $\triangle$-type three-level atom characterized by a ground state $|g\rangle$ and two excited states $|e\rangle$ and $|f\rangle$. The atom at $j=0$ resonators connects two CRWs since the cavity modes a_0 and b_0 enable the dipole-allowed transitions $|g\rangle \leftrightarrow |e\rangle$ and $|g\rangle \leftrightarrow |f\rangle$ with coupling constants g_a and g_b, respectively. A classical field with frequency $\nu = \omega_e - \omega_f$ resonantly drives the transition $|e\rangle \leftrightarrow |f\rangle$ with Rabi frequency Ω. Usually, such cyclic systems are forbidden for natural atoms, but can exist in symmetry-broken systems [11], e.g., chiral molecules [12] and artificial symmetry-broken atoms [13,14].

In the rotating frame with respect to

$$H_0 = \omega_e\Big(\sum_j a_j^\dagger a_j + |e\rangle\langle e|\Big) + \omega_f\Big(\sum_j b_j^\dagger b_j + |f\rangle\langle f|\Big),$$

the Hamiltonian of two CRWs is described by a typical tight-binding bosonic model,

$$H_c = \sum_{d=a,b}\sum_j[\Delta_d d_j^\dagger d_j - \xi_d(d_{j+1}^\dagger d_j + \text{H.c.})], \quad (1)$$

where ξ_d are the homogeneous intercavity coupling constants and $\Delta_{a(b)} = \omega_{a(b)} - \omega_{e(f)}$ are cavity-atom detunings. Hereafter d stands for $\{a, b\}$. Under the rotating-wave approximation, the interaction between the atom and two CRWs is written as

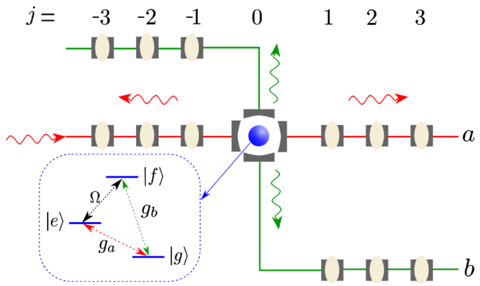

FIG. 1 (color online). Schematic of routing single photons in two channels made of two CRWs. The three-level atom characterized by $|g\rangle$, $|e\rangle$, and $|f\rangle$ is placed at the cross point $j = 0$. CRW-a (-b) couples to the atom through the transition $|g\rangle \leftrightarrow |e\rangle$ ($|g\rangle \leftrightarrow |f\rangle$) with strength g_a (g_b) and a classical field Ω is applied to resonantly drive $|e\rangle \leftrightarrow |f\rangle$ transition. An incoming wave from the left side of CRW-a is reflected, transmitted, or transferred to CRW-b.

$$H_{\text{int}} = g_a|e\rangle\langle g|a_0 + g_b|f\rangle\langle g|b_0 + \Omega|e\rangle\langle f| + \text{H.c.} \quad (2)$$

The two photonic channels are illustrated by the red and green lines in Fig. 1. Obviously, in the absence of the classical field, single photons incident from the red channel get reflected or transmitted only within the red one. Photons incident from the red channel can be switched into the other (green) channel only when $\Omega \neq 0$.

Coherent scattering of single photons.—Fourier transformation $d_k = (1/\sqrt{N})\sum_j d_j \exp(ikj)$ shows that each bare CRW supports plane waves with dispersion relation $E_k^{(d)} = \Delta_d - 2\xi_d \cos k_d$ ($k_d \in [0, 2\pi]$), i.e., each CRW possesses an energy band with the bandwidth $4\xi_d$. The detunings Δ_d and the intercavity coupling constants determine whether the two bands overlap or not. The classical field mixes the two bands.

Inside the photonic band, the incident photon with energy E will be elastically scattered. The single-excitation eigenstate is supposed to be

$$|E\rangle = U_e|e0\rangle + U_f|f0\rangle + \sum_j (A_j a_j^\dagger + B_j b_j^\dagger)|g0\rangle, \quad (3)$$

where $|0\rangle$ is the vacuum state of the CRWs and U_e, U_f, A_j, and B_j are the corresponding amplitudes. The motion of single photons are governed by the discrete scattering equations

$$ED_j = \Delta_d D_j - \xi_d(D_{j+1} + D_{j-1}) + \delta_{j0}[V_d(E)D_j + G(E)\bar{D}_j], \quad (4)$$

which is obtained from the Schrödinger equation with Hamiltonian $H = H_c + H_{\text{int}}$ by reducing the atomic amplitudes. Here, $D = \{A, B\}$ and the overbar designates the element other than D in the set $\{A, B\}$. For convenience, we have introduced the energy-dependent deltalike potentials with strength $V_d(E) = Eg_d^2/(E^2 - \Omega^2)$ and the effective dispersive coupling strength $G(E) = \Omega g_a g_b/(E^2 - \Omega^2)$ between the resonator modes a_0 and b_0. The coupling G leads to the channel switching. At $|E| = \Omega$, infinite delta potentials are formed at $j = 0$ in both CRWs. It seems that the delta potential would prevent the propagation of single photons. However, the effective coupling strength G also becomes infinite at $|E| = \Omega$, which might transfer the photon from one CRW to the other.

A wave with energy E incident from the left side of one CRW (says CRW-a) will result in reflected, transmitted, and transfer waves with the same energy. The wave functions in the asymptotic regions are given respectively by

$$A(j) = \begin{cases} e^{ik_a j} + r^a e^{-ik_a j}, & j < 0 \\ t^a e^{ik_a j}, & j > 0 \end{cases} \quad (5)$$

and

$$B(j) = \begin{cases} t_l^b e^{-ik_b j}, & j < 0 \\ t_r^b e^{ik_b j}, & j > 0 \end{cases} \quad (6)$$

where t^a (r^a) is the transmitted (reflected) amplitude and t_l^b (t_r^b) is the forward (backward) transfer amplitude. Applying solutions (5) and (6) to the discrete scattering equations (4), we obtain the scattering amplitudes,

$$t^a(E) = \frac{2i\xi_a \sin k_a[2i\xi_b \sin k_b - V_b(E)]}{\prod_{d=a,b}[2i\xi_d \sin k_d - V_d(E)] - G^2(E)}, \quad (7)$$

$$t^b(E) = \frac{2i\xi_a \sin k_a G(E)}{\prod_{d=a,b}[2i\xi_d \sin k_d - V_d(E)] - G^2(E)}, \quad (8)$$

with continuity conditions $t_r^b = t_l^b \equiv t^b$ and $t^a = r^a + 1$. Here, wave numbers k_a and k_b satisfy $E = \Delta_a - 2\xi_a \cos k_a = \Delta_b - 2\xi_a \cos k_b$. From Eqs. (7) and (8), we find that turning on the classical field makes the incoming wave in CRW-a transfer to CRW-b. It is the classical field that implements the photon-redirection function of the quantum router.

In Fig. 2, we plotted the transmittance $T^a(E) \equiv |t^a(E)|^2$, transfer rate $T^b \equiv |t^b(E)|^2$, and reflectance $R^a(E) \equiv |r^a(E)|^2$ as function of the incident energy E. Three different band configurations are presented. In Fig. 2(a), there is no overlap between two bands. In this case, single photons cannot travel in CRW-b, because k_b is complex with a positive imaginary component; i.e., single photons are localized around the atom to form local modes in CRW-b. Therefore, the photon flow is confined in CRW-a, generating the flow conservation equation $|t^a|^2 + |r^a|^2 = 1$. However, single photons in CRW-a can be perfectly reflected when their energies match the eigenvalues of the bound states of CRW-b with $g_a = 0$. In Fig. 2(b), there is the maximum overlap between two bands. In this case, the flow conservation relation changes into $|t^a|^2 + |r^a|^2 + 2|t^b|^2 = 1$. The nonvanishing transfer coefficients T^b and shows that the classical field redirects the single photons coming from one continuum to the other. In Fig. 2(c), there is partial overlap between two bands. When the energy of the incident photon is out of (within) the overlap region of

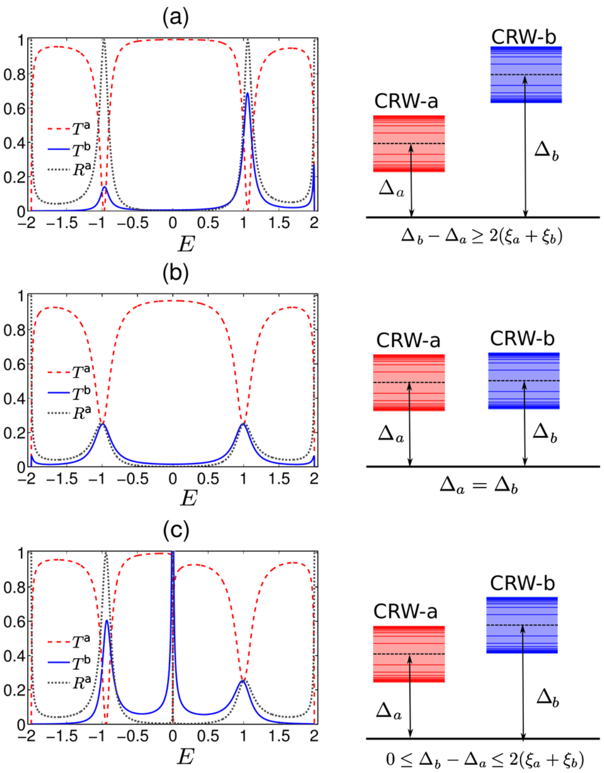

FIG. 2 (color online). The scattering process described by transmittance $T^a(E)$ (dashed red line), reflectance $R^a(E)$ (dotted gray line), and transfer rate $T^b(E)$ (solid blue line) with different configurations of the two bands of the vacant CRWs. (a) $\Delta_b = 4.5$, thus $\Delta_b - \Delta_a > 2(\xi_a + \xi_b)$; (b) $\Delta_b = 0$; (c) $\Delta_b = 2$, and then $0 < \Delta_b - \Delta_a < 2(\xi_a + \xi_b)$. For convenience, all the parameters are in units of ξ_a and we always set $\xi_b = \xi_a = 1$, $\Delta_a = 0$, $\Omega = 1$, and $g_a = g_b = 0.5$.

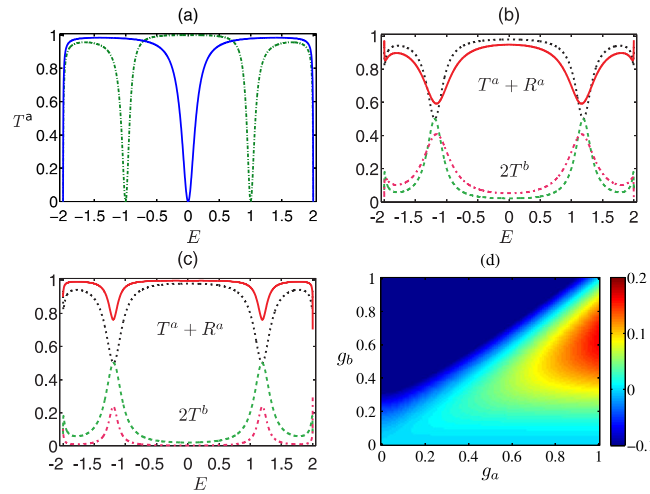

FIG. 3 (color online). (a) The transmission T^a as a function of the incident energy E with $g_a = 0.5$ and $\Omega = 0$ (solid blue line), or with $g_a = 0.5$, $g_b = 0$ and $\Omega = 1$ (dotted-dashed green line); (b),(c) The coefficients $T^a + R^a$ (solid red lines and dotted black lines), $2T^b$ (dashed green lines and dotted-dashed pink lines) as functions of the incident energy E with $g_a = 0.5$ and $\Omega = 1.2$, $g_b = 0.5$ for the dotted black and dashed green lines, or $g_b = 0.8[0.2]$ for the solid red and dotted-dashed pink lines. (d) Transmittance difference $(T^b - T^a)$ at the condition $|E| = \Omega$ vs g_a and g_b. Here, we take $\Delta_a = \Delta_b = 0$, and $\xi_a = \xi_b = 1$.

the two continuum bands, the conservation relation and the related scattering properties are the same as that in Fig. 2(a) [Fig. 2(c)]. We note that the coefficient T^b can be greater than 1 for the bound state of CRW-b. It is similar to the Feshbach resonance in cold atom scattering, the scattering cross section diverges when the energy of the incident particle matches the bound state of the closed channel. Here, the bound states in CRW-b form the closed channel-b and T^b represents the amplitude of the bound states localized around the $\triangle$ atom instead of the transmission coefficient.

Quantum routing for single photons.—To demonstrate the routing functions of our hybrid system, we first investigate the reflectance, transmittance, and transfer rate of single photons in detail when two bands are maximally overlapped.

When $\Omega = 0$, CRW-a and -b are decoupled for the case with single excitation; thus, an incoming wave is effectively scattered by a two-level atom ($|g\rangle \leftrightarrow |e\rangle$) within the incident channel. As shown in Fig. 3(a) (the solid blue line), the perfect reflection only occurs when incident waves resonate with the corresponding atomic transition [8]. The green dot-dashed line in Fig. 3(a) describes the scattering process where an incoming wave in CRW-a encounters a three-level atom in the absence of CRW-b (i.e., $g_b = 0$). It is found that the classical field makes the solid blue line split into a doublet with a separation of 2Ω. That means the incident photon resonant with the atomic transition $|e\rangle \leftrightarrow |g\rangle$, becomes transparent. Actually, $|E| = \Omega$ correspond to two dressed states of the atom interacting with the classical field. Therefore, by resonantly driving the transition $|e\rangle \leftrightarrow |f\rangle$, we are allowed to observe the electromagnetically induced transparency based on the Autler-Townes splitting [22]. When another output channel (CRW-b) exists, the conservation relation of the photon flow becomes $|t^a|^2 + |r^a|^2 + 2|t^b|^2 = 1$. In Figs. 3(b) and 3(c), the sufficiently large transfer rate T^b shows that the classical field can redirect the single photons coming from one CRW to the other and its strength Ω determines the position where the minimum of transmission in CRW-a and the maximum of the probability transferred to CRW-b occur in the energy axis. That is, $2T^b$ has two peaks centered at $E = \pm\Omega$. The height of these peaks for $2T^b$ will take maximal values when $g_a = g_b$. We can further find that the coupling strengths g_a and g_b also determine the width of each peak for $2T^b$: The larger the products $g_a g_b$ are, the wider the peaks are. The transmittance difference $T^b - T^a$ at $|E| = \Omega$ in Fig. 3(d) shows the influence of the coupling strengths g_a and g_b. Although the infinite potential $V_a(\pm\Omega)$ is supposed to totally reflect the incident single photons, the infinite coupling

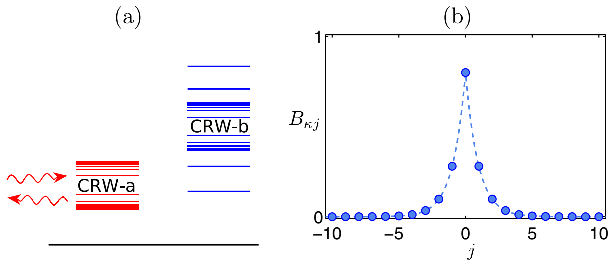

FIG. 4 (color online). (a) The CRW-b plus the $\triangle$ atom have two bound states both above and blow the continuum band. The incident photon gets perfectly reflected when its energy matches the bound states within CRW-b; (b) Wave function of the bound state within CRW-b with $n_b = 0$.

$G(\pm\Omega)$ makes the transmission zeros disappear. It can be found that, when $g_a = g_b$, $|V_a(\pm\Omega)| = |V_b(\pm\Omega)| = |G(\pm\Omega)|$ and then $T^a(\pm\Omega) = T^b(\pm\Omega)$.

Bound states.—Now we explore the underlying physical mechanism of perfect reflection in Figs. 2(a) and 2(c). Although propagating photons can get transmitted in CRW-a or reflected by the three-level atom, the perfect reflections in Fig. 2(a) do not appear at the same position as in Fig. 3(a). Here, we first study the bound states of CRW-b plus the driven $\triangle$ atom [Fig. 4(a)]. The bound states exist when the translation symmetry of the CRW-b is broken. By applying the spatial-exponential-decay solution $B_{\kappa j} = C\exp(in_b\pi j - \kappa|j|)$ ($\kappa > 0$ and $n_b = 0$, 1) as shown in Fig. 4(b) to the scattering equation Eq. (4) with $g_a = 0$, we obtain the self-consistent condition for the energies of the bound states of CRW-b,

$$(-1)^{n_b}(E^2 - \Omega^2)\sqrt{(E - \Delta_b)^2 - 4\xi_b^2} + Eg_b^2 = 0. \quad (9)$$

Solutions of Eq. (9) with $n_b = 0$ ($n_b = 1$) indicate that the eigenenergies lie below (above) the band. Thus, when the incident energies are out of the energy band of CRW-b, these photons cannot travel out of this channel, resulting in the flow conservation $|t^a|^2 + |r^a|^2 = 1$.

We note that the left-hand side of Eq. (9) is exactly the term in the square bracket of the numerator in Eq. (7) by replacing k_b with $n_b\pi + i\kappa$; i.e., the transmission zeros of T^a are completely determined by the bound states. Here, the applied classical field couples the bound states of CRW-b to the continuum of CRW-a, then bound states plus the continuum band of CRW-a form quasibound states of the total system [19]. Two interfering paths are formed: single photons travel directly through the CRW-a, or visit the bound states, return back, and continue to propagate in CRW-a. When the incident photons resonate with one of the lower two bound states, the interference originated from the interaction of a discrete localized state with a continuum of guiding modes leads to the total reflection of single photons [Fig. 4(a)]. This is different from the cases in Fig. 3 whose zeros ($T^a = 0$) result from the coherent interference between the incoming wave and the wave scattered from the atom [8]. Furthermore, this effect can be used to probe these bound states.

Conclusions.—We have studied the coherent scattering process of single photons in two 1D CRWs by a $\triangle$-type atom, which behaves as a quantum multichannel router. Here, the $\triangle$ atom functions as a single-photon switch within the incident channel in the following two ways: (1) adjusting the transition energy of the artificial atom associated with the incident channel in the absence of the classical field; (2) adjusting the configuration of the two continuums by changing the detunings to make the incident photons match the bound states of the other CRWs in the presence of the classical field. When the classical field is applied to dress the atom, single photons can be routed from one channel to the other once any dressed state matches the continuums of the two channels. The promising candidates for experimental implementations of the above quantum routing system are the following: The circuit QED system [23] where two coplanar linear resonators are coupled to a cyclic $\triangle$-atom [14] using three Josephson junctions and microwaves serve as the classical controlling field; The defect cavities in photonic crystal coupled to a silicon-based quantum dot [24,25]. We hope that the quantum routing function predicted in this letter can be observed in some experiments.

This work is supported by NSFC No. 11074071, No. 11374095, No. 11121403, No. 10935010, No. 11174027, and No. 11074261; NFRPC No. 2012CB922103, and No. 2012CB922104, No. 2014CB921402, Hunan Provincial Natural Science Foundation of China (11JJ7001, 12JJ1002), and Scientific Research Fund of Hunan Provincial Education Department (No. 11B076).

*cpsun@csrc.ac.cn; http://www.csrc.ac.cn/~suncp

[1] T. Aoki, A. Parkins, D. Alton, C. Regal, B. Dayan, E. Ostby, K. Vahala, and H. Kimble, Phys. Rev. Lett. **102**, 083601 (2009).
[2] I.-C. Hoi, C. M. Wilson, G. Johansson, T. Palomaki, B. Peropadre, and P. Delsing, Phys. Rev. Lett. **107**, 073601 (2011).
[3] G. S. Agarwal and S. M. Huang, Phys. Rev. A **85**, 021801 (R) (2012).
[4] X.-S. Ma, S. Zotter, J. Kofler, T. Jennewein, and A. Zeilinger, Phys. Rev. A **83**, 043814 (2011).
[5] X.-Y. Chang *et al.*, arXiv:1207.7265.
[6] J. T. Shen and S. Fan, Phys. Rev. Lett. **95**, 213001 (2005); Phys. Rev. A **79**, 023837 (2009); **79**, 023838 (2009); S. Fan, P. Villeneuve, J. Joannopoulos, M. Khan, C. Manolatou, and H. Haus, Phys. Rev. B **59**, 15882 (1999).
[7] J. T. Shen and S. Fan, Phys. Rev. Lett. **98**, 153003 (2007); T. Shi and C. P. Sun, Phys. Rev. B **79**, 205111 (2009); T. Shi, Shanhui Fan, and C. P. Sun, Phys. Rev. A **84**, 063803 (2011);
[8] L. Zhou, Z. R. Gong, Y.-x. Liu, C. P. Sun, and F. Nori, Phys. Rev. Lett. **101**, 100501 (2008); Phys. Rev. A **80**,

062109 (2009); **85**, 013806 (2012); J.-Q. Liao, Z. R. Gong, L. Zhou, Y.-x. Liu, C. P. Sun, and F. Nori, Phys. Rev. A **81**, 042304 (2010); H. Dong, Z. R. Gong, H. Ian, L. Zhou, and C. P. Sun, Phys. Rev. A **79**, 063847 (2009).

[9] P. Longo, P. Schmitteckert, and K. Busch, Phys. Rev. Lett. **104**, 023602 (2010).

[10] Z. R. Gong, H. Ian, L. Zhou, and C. P. Sun, Phys. Rev. A **78**, 053806 (2008); T. S. Tsoi and C. K. Law, Phys. Rev. A **80**, 033823 (2009).

[11] Y. Li, L. Zheng, Y.-x. Liu, and C. P. Sun, Phys. Rev. A **73**, 043805 (2006).

[12] P. Král and M. Shapiro, Phys. Rev. Lett. **87**, 183002 (2001); P. Král, I. Thanopulos, M. Shapiro, and D. Cohen, *ibid.* **90**, 033001 (2003).

[13] Y. Li, C. Bruder, and C. P. Sun, Phys. Rev. Lett. **99**, 130403 (2007).

[14] Y.-x. Liu, J. Q. You, L. F. Wei, C. P. Sun, and F. Nori, Phys. Rev. Lett. **95**, 087001 (2005).

[15] P. W. Anderson, Phys. Rev. **124**, 41 (1961).

[16] U. Fano, Phys. Rev. **124**, 1866 (1961).

[17] H. Friedrich and D. Wintgen, Phys. Rev. A **32**, 3231 (1985).

[18] H. Nakamura, N. Hatano, S. Garmon, and T. Petrosky, Phys. Rev. Lett. **99**, 210404 (2007).

[19] D. Z. Xu, H. Ian, T. Shi, H. Dong, and C. P. Sun, Science China Physics, Mechanics and Astronomy **53**, 1234 (2010).

[20] J. M. Zhang, D. Braak, and M. Kollar, Phys. Rev. Lett. **109**, 116405 (2012); Phys. Rev. A **87**, 023613 (2013).

[21] J. von Neumann and E. Wigner, Phys. Z. **30**, 467 (1929).

[22] J. Li *et al.*, Sci. Rep. **2**, 645 (2012); J. Li, G. S. Paraoanu, K. Cicak, F. Altomare, J. I. Park, R. W. Simmonds, M. A. Sillanpää, and P. J. Hakonen, Phys. Rev. B **84**, 104527 (2011).

[23] A. Wallraff, D. I. Schuster, A. Blais, L. Frunzio, R.-S. Huang, J. Majer, S. Kumar, S. M. Girvin, and R. J. Schoelkopf, Nature (London) **431**, 162 (2004); D. I. Schuster *et al.*, *ibid.* **445**, 515 (2007); A. Blais, J. Gambetta, A. Wallraff, D. Schuster, S. Girvin, M. Devoret, and R. Schoelkopf, Phys. Rev. A **75**, 032329 (2007).

[24] M. Notomi, E. Kuramochi, and T. Tanabe, Nat. Photonics **2**, 741 (2008).

[25] G. Khitrova, H. M. Gibbs, M. Kira, S. W. Koch, and A. Scherer, Nat. Phys. **2**, 81 (2006).